INTERNATIONAL JOURNAL of RENEWABLE ENERGY RESEARCH
K. I. Mahider et al., Vol.16, No.2, June, 2026

Design and Simulation of Novel Control Strategy of STATCOM Tuned by Combined Hybrid GA-PSO Algorithm

Khadija-Ikram Mahider*‡, Reda Rabeh**, Mohammed Ferfra*

* Engineering for Smart and Sustainable Systems Research Center, Mohammadia School of Engineers, Mohammed V University in Rabat, Ibn Sina, Rabat, 10000, Morocco.

** LERMA Laboratory, College of Engineering, International University of Rabat, Sala Al Jadida,11100, Morocco

(khadija-ikram.mahider@research.emi.ac.ma, reda.rabeh@uir.ac.ma, ferfra@emi.ac.ma)

‡Corresponding Author; Khadija-Ikram Mahider, N°02, Rue 80, Avenue Jamia Arabia, Hay Hassani, Dakhla Oued Eddahab, Morocco, Tel: +212 676 394 841, khadija-ikram.mahider@research.emi.ac.ma

Received: 14.03.2024 Accepted: 05.05.2024

Abstract- Voltage stability is a critical and important issue in power grid operation. STATCOM, as an adaptive FACTS controller, provides limited range linear control for non-linear processes. The major objective of the study presented in this paper is to prove and highlight the accuracy of the novel proposed control strategy of STATCOM optimized by combining classical evolutionary algorithms. The approach adopted for the STATCOM is a composition of existing controllers, PI, and Fractional PI. The novel control strategy aims to propose controllers in different loops tuned by evolutionary algorithms. These selected methods are particle swarm optimization (PSO), genetic algorithms (GA), and a hybrid combination of PSO and GA, which were adopted to tune the studied STATCOM control parameters in different strategies. Simulation results of this article are obtained using the Simulink environment. These results demonstrate the accuracy of the optimized two PI-PIFOPI STATCOM (PI controller in the outer loops of DC and AC voltage loops and cascaded PI and FOPI in the internal current loop) in stabilizing the grid voltage. This optimization was adopted by minimizing the objective selected in this study, the function ISE (Integral of the Squared Error) of grid voltage. The robustness and the accuracy of the proposed STATCOM are proved by random variation of the studied system parameters.

Keywords STATCOM, voltage stability, GA-PSO, PI controller, FOPI controller, PIFOPI.

1. Introduction

The voltage profile must be improved to ensure stability of the distributed electrical grids and ensure different parts of power quality. Today, voltage instability and line overload are the main problems in electricity systems. Voltage stability is thoroughly analyzed by examining the production, transmission, and consumption. Since reactive power is unbalanced, there is instability in the voltage profile. FACTS power electronic device has been developed to improve the power transfer in the grid and ensure voltage stability [1]. FACTS controls power flow, voltage regulation, transient and dynamic stability performances, and vibration damping in transmission lines [2].

FACTS are classified into three types according to reference [3], which are: TSSC, TCSC, TSSR, and TCSR, as series connected FACTS; TCR, SVC, and STATCOM as shunt connected FACTS; and UPFC as combined hybrid connected FACTS. STATCOM and SVC as shunt-connected controllers are considered the most powerful type of FACTS to control the grid voltage. The impact of these FACTS is highlighted in [4-5]. In fact, the STATCOM topology may offer more powerful damping performances than the SVC. Reference [5] describes both operating modes of STATCOM (inductive and capacitive modes). These modes depend on the grid voltage value. In fact, the classical implemented controller is the PID as a linear controller. The dynamic performances of this controller can be improved by a well-tuning of its parameters using evolutionary algorithms [6-7].

The literature contains many optimization techniques and evolutionary strategies. Bee Colony Optimization (BCO) is an optimization method stimulated by honeybees' foraging behaviour. This optimization was applied in tuning the PID controller as highlighted in [8].

The comparative study of the Teacher Learning Based Optimization (TLBO) algorithms. TLBO highlights the improved performances of students under teacher influence. Then, the Cuckoo Search Algorithm (CSA) is inspired by the obligatory cuckoo parasite. The study demonstrates the efficiency of the TLBO compared to the CSA in optimizing the voltage management parameters for the control system [9].

The PSO algorithm was operated to design the PI (proportional-integral) regulator in [10]. The optimization results prove the good dynamic at different reference values with this PI-PSO tuned controller. A comparative study was done in reference [11]. The main idea is to perfectly design the STATCOM controller using the combination of the WCA-PSO algorithm of PSO and the Water Cycle Algorithm (WCA). High performances of the hybrid WCA-PSO were highlighted compared to WCA and PSO in tuning the STATCOM controller.

In reference [12], another study with Genetic Algorithms (GA), the PSO algorithm, and the hybrid combination GA-PSO to optimize controller parameters. PSO is based on the social behavior of swarm-living animals. GA is an optimization approach according to genetic process and natural selection principles. This comparison clearly showed that the hybrid GA-PSO algorithm performs in comparison with different classic, commonly used algorithms presented in the main work of this research paper.

Following the exciting studies in the literature. In this work, we were interested in finding a good control strategy to control our voltage regulator. The main contributions of this research are:

- Demonstrate the proposed STACOM control strategy of the voltage regulator in the studied power system using cascade implementation of FOPI and PI controller in different control loops.
- Validate the hybrid algorithm GA-PSO to optimize the gains of the proposed structures regulator of the considered system.
- Prove the efficiency and the accuracy of the proposed STATCOM control strategy.

The main plan of this research paper is presented as follows: The second section describes the different units used in the studied model. The different controllers studied, and the propped control strategy will be well described in the third section presented. The fourth section illustrates the tuning technique and control strategies used to obtain dynamic solutions for higher power quality. The fifth section presents the simulation results using the Simulink environment. The sixth section concludes with the entire research paper.

2. STATCOM Model Adopted in Electrical Grid

A distributed power grid with a nominal frequency of 50 Hz and a nominal voltage of 230 kV supplies both fixed and variable loads, as illustrated in the studied system presented in this research paper. Figure 1 shows a STATCOM used as a shunt-connected FACTS device, interfaced with the grid through an 8500 MVA YY transformer.

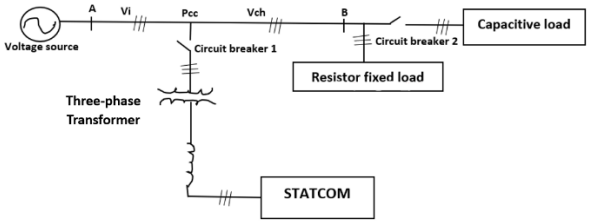

Fig. 1. Block diagram of a three-phase voltage flicker compensation system in the studied grid.

2.1. Simplified Mathematical Model

The STATCOM, considering only the busbar to which it is connected. The equivalent model presented in Figure 3:

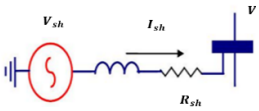

Fig. 2. Representative circuit of the adopted STATCOM connected to the grid.

The simplified STATCOM model assumes that the DC circuit consists of a constant voltage source, and the DC circuit is not considered in this model. The equivalent diagram of this device is therefore a sinusoidal voltage source connected to the nodes of the network through the inductance L_{sh} via a coupling transformer (Fig. 2). The circuit also includes series resistors representing the ohmic losses R_{sh} in the transformer and the losses in the inverter switches [13-14].

The STATCOM current is calculated by the difference between two voltage values: the system voltage V (node voltage) and the controllable STATCOM voltage.

Using Ohm's law, we get

$$\begin{bmatrix} V_a \\ V_b \\ V_c \end{bmatrix} - \begin{bmatrix} V_{ash} \\ V_{bsh} \\ V_{csh} \end{bmatrix} = R_{sh} \begin{bmatrix} I_{ash} \\ I_{bsh} \\ I_{csh} \end{bmatrix} + L_{sh} \frac{d}{dt} \begin{bmatrix} I_{ash} \\ I_{bsh} \\ I_{csh} \end{bmatrix} \quad (1)$$

To simplify these equations, we pass to the fixed orthogonal reference (d, q) we multiply the equation (1) by the matrix of the following Clark-Park transformation we find:

$$\bar{V}^{(d\,q)}.e^{j\gamma} - \overline{V_{sh}}^{(d\,q)}.e^{j\gamma} = R_{sh}\overline{I_{sh}}^{(d\,q)}.e^{j\gamma} + L_{sh}\frac{d}{dt}\left(\overline{I_{sh}}^{(d\,q)}.e^{j\gamma}\right) \quad (2)$$

The simplified dynamic model of STATCOM in reference (d, q) is defined as:

$$V_{dq} - V_{sh} = R_{sh}I_{sh} + L_{sh}\frac{dI_{sh}}{dt} - L_{sh}.\omega \begin{bmatrix} 0 & 1 \\ 1 & 0 \end{bmatrix} I_{sh} \quad (3)$$

In the form of a matrix, the system of states of the STATCOM is written as follows:

$$\frac{d}{dt}\begin{bmatrix} I_{shd} \\ I_{shq} \end{bmatrix} = \begin{bmatrix} -\frac{R_{sh}}{L_{sh}} & \omega \\ -\omega & -\frac{R_{sh}}{L_{sh}} \end{bmatrix} \cdot \begin{bmatrix} I_{shd} \\ I_{shq} \end{bmatrix} + \frac{1}{L_{sh}} \cdot \begin{bmatrix} V_d & -V_{shd} \\ V_q & -V_{shq} \end{bmatrix} \quad (4)$$

Where the vector $\begin{bmatrix} V_d & -V_{shd} \\ V_q & -V_{shq} \end{bmatrix}$ corresponds to the control law vector of the studied system in this paper.

2.2. Dynamic Model of the DC Circuit

In the simulated mode, an assumption was applied that the DC voltage U_{dc} doesn't depend on small active energy transfer between the DC source of STATCOM and the grid. With the assumption of the waw value pf the capacitance of the DC source, the mathematical model should be improved by the DC circuit equation [13].

The DC circuits connect a DC source to a capacitor and a shunt resistor [14]. Figure 3 illustrates the equivalent circuit of STSTCOM with a DC circuit.

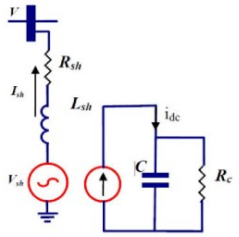

Fig. 3. Representative circuit of the studied STATCOM with DC circuit.

We suppose that:

$$V_{sh}^{(d\,q)} = V_{shd} + j\,V_{shq} = v * [\cos(\theta) + j\,\sin(\theta)] \quad (5)$$

v: is the modulus of the injection voltage, depending on the DC voltage value U_{dc}. The expression of v is:

$$v = m \times U_{dc} \quad (6)$$

m: the modulation index referring to the inverter.

So, the V_d and V_q components are given by the equation:

$$V_{dq} - mU_{dc}e^{j\theta} = R_{sh}I_{sh} + L_{sh}\frac{dI_{sh}}{dt} - L_{sh}.\omega\begin{bmatrix} 0 & 1 \\ 1 & 0 \end{bmatrix} I_{shq} \quad (7)$$

The expression of the tie power between the voltage inverter and the capacitor is:

$$P_{sh} = \frac{3}{2}\left(V_{shd}I_{shd} + V_{shq}Ishq\right) \quad (8)$$

$$U_{dc}I_{dc} = \frac{3}{2}\left(V_{shd}I_{shd} + V_{shq}Ishq\right) \quad (9)$$

The differential equation of the DC part of the STATCOM is:

$$C\frac{dU_{dc}}{dt} = \frac{3}{2}\,m\left(I_{shd}\cos(\theta) - I_{shq}\sin(\theta)\right) - \frac{U_{dc}}{R_{dc}} \quad (10)$$

The matrix form of STATCOM state equations considering variations in the output voltage value obtained from the DC circuit is written:

$$\frac{d}{dt}\begin{bmatrix} I_{shd} \\ I_{shq} \\ U_{dc} \end{bmatrix} = A\begin{bmatrix} I_{shd} \\ I_{shq} \\ U_{dc} \end{bmatrix} + B\begin{bmatrix} V_d \\ V_q \end{bmatrix} \quad (11)$$

Were:

$$A = \begin{bmatrix} -\frac{R}{L_{sh}} & \omega & -\frac{m}{L_{sh}}\cos\theta \\ -\omega & -\frac{R}{L_{sh}} & \frac{m}{L_{sh}}\sin\theta \\ \frac{3}{2}\frac{m}{c}\cos\theta & -\frac{3}{2}\frac{m}{c}\cos\theta & -\frac{1}{R_{dc}c} \end{bmatrix}, \quad B = \begin{bmatrix} \frac{1}{L_{sh}} & 0 \\ 0 & \frac{1}{L_{sh}} \\ 0 & 0 \end{bmatrix}$$

In this system, three state parameters to control, two control parameters, and two quantities can be controlled independently. This system is linear around an operating point; it can be expressed as follows:

$$\frac{d}{dt}\begin{bmatrix} I_{shd} \\ I_{shq} \\ U_{dc} \end{bmatrix} = A'\begin{bmatrix} I_{shd} \\ I_{shq} \\ U_{dc} \end{bmatrix} + B'\begin{bmatrix} V_d \\ V_q \\ \theta \end{bmatrix} \quad (12)$$

Were:

$$A' = \begin{bmatrix} -\frac{R}{L_{sh}} & \omega & -\frac{m}{L_{sh}}\cos\theta_0 \\ -\omega & -\frac{R}{L_{sh}} & \frac{m}{L_{sh}}\sin\theta_0 \\ \frac{3}{2}\frac{m}{c}\cos\theta_0 & -\frac{3}{2}\frac{m}{c}\cos\theta_0 & -\frac{1}{R_{dc}c} \end{bmatrix}$$

$$B' = \begin{bmatrix} \frac{1}{L_{sh}} & 0 & \frac{m}{L_{sh}}U_{dc0}\sin\theta_0 \\ 0 & \frac{1}{L_{sh}} & \frac{m}{L_{sh}}U_{dc0}\cos\theta_0 \\ 0 & 0 & -\frac{2}{3}\frac{m}{c}I_{shd}\left(\sin\theta + I_{shq}\cos\theta_0\right) \end{bmatrix}$$

The reactive part of the STATCOM current is controlled separately to manage and deal with the flow of reactive power. The remaining parameters are employed to maintain and ensure transient and steady-state stability of the DC voltage U_{dc} [14].

3. State of the Art of the Different Controllers

3.1. PI Controller

The PI controller is defined by two terms or two main actions, namely proportional and integral control [15]. The formulation of the controller law of the classical PI controller is expressed in an equation (13), and its general structure is presented in Fig 4.

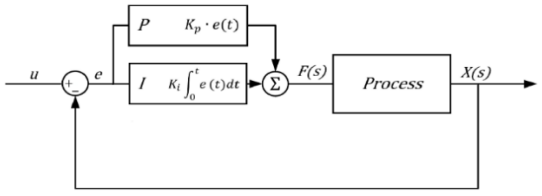

Fig. 4. General structure of a PI.

The PI controller law in Laplace form can be expressed by:

$$C(S) = K_p + K_i\,\frac{1}{s} \quad (13)$$

3.2. Fractional PI Controller (PI^{λ})

Podlubny offers the PI^{λ} regulator to ameliorate and adjust the behavior of the linear PI controller, using an integrator of order λ, where λ belongs to the set of real numbers. It's considered an extension of classical control theory.

The main positive performance of the PI^{λ} controller is its ability to control the dynamics of fractional order systems. It's also known by its smaller sensitivity to changes in the parameters of a controlled system. That's why it provides an improvement in robustness regarding the integer controller.

Compared to PI, the PI^{λ} provides more flexibility thanks to an additional degree of freedom that allows for precise tuning of the dynamic properties of fractional-order regulation loops. [16]. The following figure illustrates the PI^{λ} controller [16].

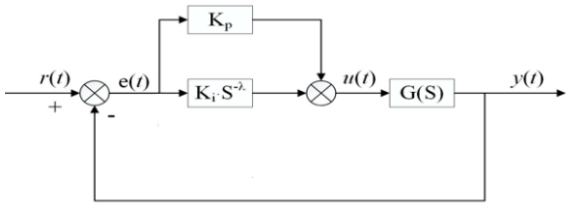

Fig. 5. Schematic structure of a PI^{λ}.

The equation of the controller law of the PI^{λ} controller of fractional order in the time domain is given in the following equation:

$$u(t) = k_i\, D^{-\lambda}\, e(t) + k_p e(t) \tag{14}$$

The transfer function of this corrector in the Laplace domain can be expressed by:

$$C(S) = k_p + k_i \frac{1}{s^{\lambda}} \tag{15}$$

3.3. Two PI Controllers in Cascade

Based on these controllers, a cascaded combination of two PI controllers can be proposed and studied as illustrated in Figure 6.

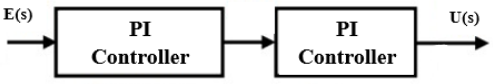

Fig. 6. Diagram of two PI controllers in cascade.

The expression of the control law of this specific controller is formulated as:

$$C(S) = C_{PI1}(S) \times C_{PI2}(S) \tag{16}$$

$$C(S) = \left(K_{p1} + K_{i1}\frac{1}{s}\right)\left(\mathrm{K_{p2}} + K_{i2}\frac{1}{s}\right) = \alpha_1 + \alpha_2.\frac{1}{s} + \alpha_3.\frac{1}{s^2} \tag{17}$$

With (k_{i1}, k_{i2}) and (k_{p1}, k_{p2}) representing the integral and the proportional parameters or gains of the two combined PI controllers.

Where:

$$\alpha_1 = k_{p1} * k_{p2};\ \alpha_2 = k_{p2} * k_{i1} + k_{p1} * k_{i2};\ \alpha_3 = k_{i1} * k_{i2}$$

3.4. PI Controller in Cascade with Fractional PI (PIFOPI)

The proposed approach in this paper is a cascade composition of the two controllers: PI and FOPI. It is clearly illustrated in the figure below:

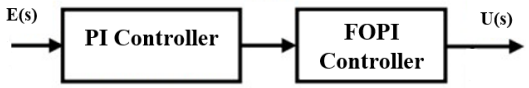

Fig. 7. Schematic Diagram of cascaded PI and FOPI controllers.

The formulation of the control law of the combined PI-FOPI controller is:

$$C(S) = C_{PI}(S) \times C_{FOPI}(S) \tag{18}$$

$$C(S) = \left(k_{p1} + k_{i1}\frac{1}{s}\right)\left(\mathrm{k_{p2}} + k_{i2}\frac{1}{s^{\lambda}}\right) = \alpha_1 + \alpha_2.\frac{1}{s} + \alpha_3.\frac{1}{s^{\lambda}} + \alpha_4.\frac{1}{s^{\lambda+1}} \tag{19}$$

(K_{i1}, K_{i2}) and (K_{p1}, K_{p2}) represent the integral and the proportional parameters or gains of the proposed controller with combined PI and FOPI controllers.

Where:

$$\alpha_1 = K_{p1}.K_{p2}\ ;\ \alpha_2 = K_{p2}.K_{i1};\ \alpha_3 = K_{p1}.K_{i2};\ \alpha_4 = K_{i1}.K_{i2}$$

4. STATCOM Control Strategies

Applying Park transformation to the STATCOM voltage V_{abc} and current I_{abc} to (q,d) domain, the amplitude $MagV$ is expressed as:

$$MagV = \sqrt{\left(V_d^2 + V_q^2\right)} \tag{20}$$

$$\begin{cases} I_{qref} = Q_{ref} \times \dfrac{1}{MagV}\ ;\ \text{If}: MagV \neq 0 \\ I_{qref} = \dfrac{Q_{ref}}{10^{-6}};\ \text{If}: MagV = 0 \end{cases} \tag{21}$$

The following figure describes the architecture of different loops of STATCOM.

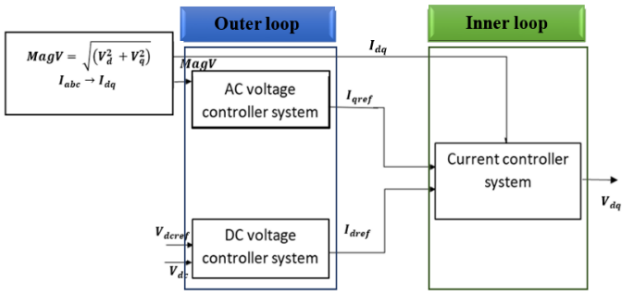

Fig. 8. STATCOM controller schematic.

The global architecture of a STATCOM is presented by two systems with two connected loops: the outer or external loop that contains the DC and AC voltage loops, and an inner

or internal loop that controls the current. To guarantee the robustness and effectiveness of the main contribution of this research paper, the internal system must be faster than the external system.

4.1. Scenario 1: 3PI

In this scenario, we apply the PI controller in the external loop (the DC and AC voltage control loops) and internal loop presented by the two current control loops. Then, the main objective of the AC voltage regulator is to generate the updated I_{qref} value as expressed in the following two equations:

$$I_{qref} = \left(k_{pAC} + \frac{k_{iAC}}{s}\right) * \left(Q_{ref} - Qmeas\right) \quad (22)$$

Or:

$$I_{qref} = \left(k_{pAC} + \frac{k_{iAC}}{s}\right) * \left(V_{acref} - MagV\right) \quad (23)$$

The main objective of DC voltage regulator is to generate the updated value of the direct current I_{dref}. The following Eq. (24) expresses this reference value of I_{dref} as:

$$I_{dref} = \left(k_{pDC} + \frac{k_{iDC}}{s}\right) * \left(V_{dcref} - V_{dc}\right) \quad (24)$$

The internal controllers of direct and quadratic current aim to provide the two components of the controller law V_d and V_q. They are formulated as:

$$V_d = \left(k_{pI} + \frac{k_{iI}}{s}\right) * \left(I_d - I_{dref}\right) \quad (25)$$

$$V_q = \left(k_{pI} + \frac{k_{iI}}{s}\right) * \left(I_q - I_{qref}\right) \quad (26)$$

4.2. Scenario 2: 2PI+PI in Cascade

In this scenario, we apply the PI controller in the outer system (the DC and AC voltage control loops) and two cascaded PI controllers in the internal loop (current control loop).

The expression of the quadratic component of the current I_{qref} as the output value of the controller of the AC voltage loop is:

$$I_{qref} = \left(k_{pAC} + \frac{k_{iAC}}{s}\right) * \left(Q_{ref} - Qmeas\right) \quad (27)$$

Or:

$$I_{qref} = \left(k_{pAC} + \frac{k_{iAC}}{s}\right) * \left(V_{acref} - MagV\right) \quad (28)$$

In this strategy, I_{dref} is expressed by the equation:

$$I_{dref} = \left(k_{pDC} + \frac{k_{iDC}}{s}\right) * \left(V_{dcref} - V_{dc}\right) \quad (29)$$

The expressions of V_d and V_q are given in the two following equations:

$$V_d = \left(\frac{K_{iI1}}{s} + K_{pI1}\right) * \left(\frac{K_{iI2}}{s^{\lambda}} + K_{pI2}\right) * \left(I_d - I_{dref}\right) \quad (30)$$

$$V_q = \left(\frac{K_{iI1}}{s} + K_{pI1}\right) * \left(\frac{K_{iI2}}{s^{\lambda}} + K_{pI2}\right) * \left(I_q - I_{qref}\right) \quad (31)$$

4.3. Scenario 3: 2PI+FOPI

In this scenario, we use the PI controller in the outer system loop (the AC voltage control and DC voltage control loops) and the fractional PI (FOPI) in the internal system loop (current control loop).

Using this control approach, the updated expressions of the quadratic current I_{qref} is expressed as:

$$I_{qref} = \left(k_{pAC} + \frac{k_{iAC}}{s}\right) * \left(Q_{ref} - Qmeas\right) \quad (32)$$

Or:

$$I_{qref} = \left(k_{pAC} + \frac{k_{iAC}}{s}\right) * \left(V_{acref} - MagV\right) \quad (33)$$

The formulation of the direct current component I_{dref} is presented in the following equation:

$$I_{dref} = \left(k_{pDC} + \frac{k_{iDC}}{s}\right) * \left(V_{dcref} - V_{dc}\right) \quad (34)$$

In this case, the expressions of V_d and V_q are given in the two following equations:

$$V_d = \left(\frac{k_{iI}}{s^{\lambda}} + k_{pI}\right) * \left(I_d - I_{dref}\right) \quad (35)$$

$$V_q = \left(\frac{k_{iI}}{s^{\lambda}} + k_{pI}\right) * \left(I_q - I_{qref}\right) \quad (36)$$

4.4. Scenario 4 :2PI+PIFOPI

This scenario presents the proposed controller of the studied system in this paper. The external controller loop presented by the PI controller is basically in the control systems: the AC and DC voltage loops. In the internal system presented by the current control loop, a cascade combination of PI and FOPI controllers is adopted. Then, the expression of direct and quadratic currents I_{qref} and I_{dref} is given in the following equations:

$$I_{qref} = \left(k_{pAC} + \frac{k_{iAC}}{s}\right) * \left(Q_{ref} - Qmeas\right) \quad (37)$$

Or:

$$I_{qref} = \left(k_{pAC} + \frac{k_{iAC}}{s}\right) * \left(V_{acref} - MagV\right) \quad (38)$$

$$I_{dref} = \left(k_{pDC} + \frac{k_{iDC}}{s}\right) * \left(V_{dcref} - V_{dc}\right) \quad (39)$$

Using the proposed control in STATCOM, the expressions of V_d and V_q are given in the following two equations:

$$V_d = \left(K_{pI1} + \frac{K_{iI1}}{s}\right) * \left(K_{pI2} + \frac{K_{iI2}}{s^{\lambda}}\right) * \left(I_d - I_{dref}\right) \quad (40)$$

$$V_q = \left(K_{pI1} + \frac{K_{iI1}}{s}\right) * \left(k_{pI2} + \frac{K_{iI2}}{s^{\lambda}}\right) * \left(I_q - I_{qref}\right) \quad (41)$$

4.5. Optimization Method

We optimize the PI controller parameters using evolutionary techniques, in particular, two algorithms, PSO and GA. These approaches will be compared to the hybrid

GA-PSO approach that combines both methods. The tuning process aims to minimize a fitness function, where variable X is defined by the different parameters of inner and outer controllers according to each scenario. In fact, X is constrained between a lower bound (VarMin) and an upper bound (VarMax). The objective function can be one of the four following errors:

The integral of the squared error value (ISE):

$$\int \left(V - V_{ref}\right)^2 dt \quad (42)$$

The integral of the absolute error value (IAE):

$$\int \left|V - V_{ref}\right| dt \quad (43)$$

The integral time of the squared error value (ITSE):

$$\int t \left(V - V_{ref}\right)^2 dt \quad (44)$$

The integral time absolute error value (ITAE):

$$\int t\left|V - V_{ref}\right| dt \quad (45)$$

4.5.1. Genetic algorithm (GA)

The American scientist John Henry Holland developed the Genetic Algorithm (GA) in the 1970s. It is a metaheuristic from the large family of evolutionary algorithms, which provides very high-quality solutions in a reasonable time, by maximizing or minimizing the objective function. The inspiration for this algorithm comes from the process of evolution of living beings.

In the beginning, GA starts with a generated population of candidate solutions. These potential solutions progressively evolve across successive generations until an optimal or near-optimal set of solutions is obtained. Each candidate of the population has properties and can undergo genetic transformations (mutation, crossing, selection, and reproduction). Then, it is evaluated, and this fitness value is a criterion for its survival from one generation to the next [17-18].

To reach the best value of the classical PI controller gains of all STATCOM loops in this work, we use the genetic algorithm. Figure 9 shows the presented GA flowchart [18].

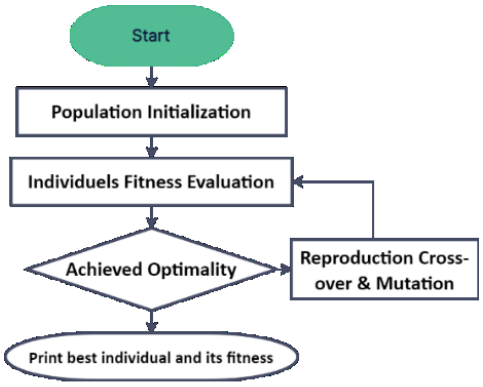

Fig. 9. Flow chart of GA.

4.5.2. Particle swarm optimization (PSO)

PSO is an optimization approach implemented and inspired by the social behavior of animals. It is based on how groups like fish schools and bird flocks move and interact. It is a stochastic approach initially developed and performed by the two researchers Eberhart and Kennedy in 1995 [19]. This evolutionary optimization approach deals with a group of individuals called particles. Initially, these particles are randomly distributed. They then move through the search space to find optimal solutions. In fact, in this method, each particle presents a potential. It has a position X_k^i and a velocity V_k^i. The best position of each particle is memorized in P_k^i. In addition, it is deeply dependent on the best position of the group named P_k^g. The evolution equations of this optimization algorithm in the continuous case. It's determined as follows: [20-21].

$$V_{k+1}^i = \omega * V_k^i - \left[C_1 r_1 \left(X_k^i - P_k^i\right) + C_2 r_2 \left(X_k^g - P_k^g\right)\right] \quad (46)$$

$$X_{k+1}^i = V_{k+1}^i + X_k^i \quad (47)$$

Note that ω designates the coefficient of inertia, the coefficients C_1 and $C_2$are constants determined empirically according to the relation C1 + C2 ≤ 4, and finally, r_1 and r_2 are random positive numbers which follow a uniform distribution in the interval between 0 and 1 [20-21]. The detailed steps of the PSO algorithm are illustrated in Figure 10 [22].

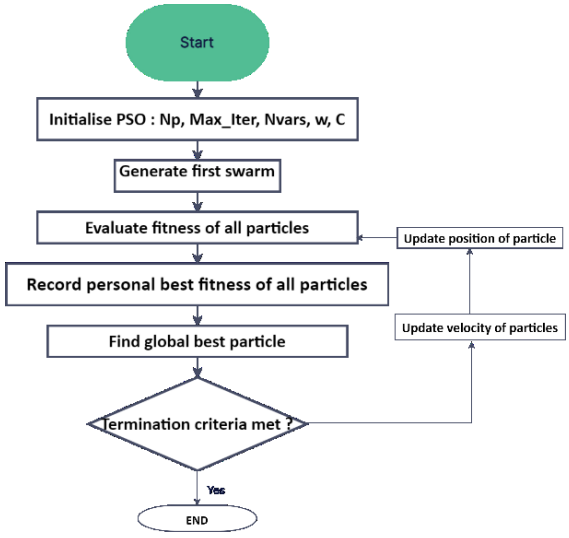

Fig. 10. PSO flowchart.

4.5.3. Hybrid combined algorithm GA-PSO

The proposed method in this paper is named hybrid PSO-GA. This approach aims to select and combine the performances of GA and PSO. In fact, GA-PSO merges the global search performances of GA and the local search performances of PSO to reach a global optimum solution. In this proposed approach, the random generation of the different parameters of PSO is considered. It deals with particles moving in a search space. Each particle has a velocity. The velocity vector is important to update each particle's position. Depending on the defined design variables, the updated position is calculated. The swarm adjusts its position

according to the two important pieces of information: the memory of each particle and shared information. Finally, the creation of a new generation is done by applying GA for selecting new particles. Taking into consideration time constraints, the application of the GA process doesn't cover the entire population [23].

$$GA_{Num} = GA_{NumMax} - \left(\frac{PSO_i}{PSO_{MaxIter}}\right)^{\gamma} \times B \quad (48)$$

Where: $B = GA_{NumMax} - GA_{NumMin}$

The current or the last PSO iteration is presented by PSO_i and is the maximum iteration number, $PSO_{MaxIter}$.

The main concept of the proposed method is the implementation of the genetic principles to reach the best individuals. It depends on the three operations: selection, crossover, and mutation.

$$\begin{cases} y_i & if\ f(y_i) < f(x_i) \\ x_i & otherwise\ i = 1, 2, \ldots GA_{PS} \end{cases} \quad (49)$$

After evaluating the new population, the population size and the maximum number of GA iterations are adjusted according to the PSO iteration, and their connection is well presented and defined as follows:

$$GA_{PS} = GA_{MinPS} - \left(\frac{PSO_i}{PSO_{MaxIter}}\right)^{\gamma} \times B1 \quad (50)$$

$$GA_{MaxIter} = GA_{MinIter} - \left(\frac{PSO_i}{PSO_{MaxIter}}\right)^{\beta} \times B2 \quad (51)$$

Where: $B_1 = GA_{NumMax} - GA_{NumMin}$ and $B_2 = GA_{MaxIter} - GA_{MinIter}$.

Figure 11 illustrates the different steps of the proposed optimization approach.

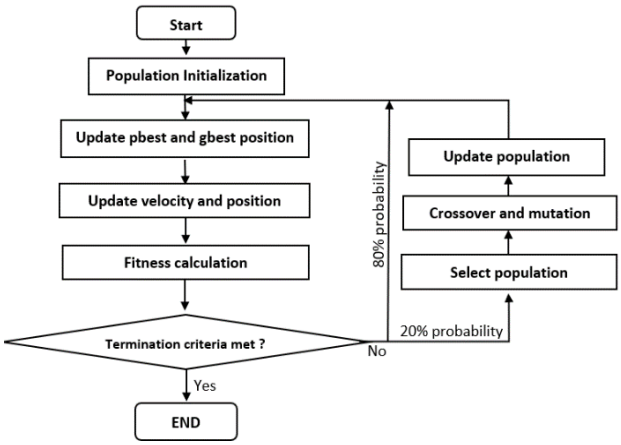

Fig. 11. Simplified flowchart of the proposed hybrid combination of two algorithms, GA-PSO.

5. Results and Discussion

The studied system in this work deals with a variable load. It's defined by a fixed resistive load (active) with a rated active power of 20 MW and an inductive (reactive) load with a rated reactive power of 150 MVAR, which is activated between t=0.2s and t=0.4s.

In order to determine the best STATCOM control strategy parameters, we minimize the objective function using the previous optimization algorithms for each proposed control strategy. Tables 1 and 2 respectively give the parameters fixed and adopted to run the two algorithms of the GA and PSO used in this work to run these algorithms.

Table 1. GA program parameters

Parameter	Variable	Values
Extra Range Factor for Crossover	γ	0,4
Crossover Percentage	P_c	0,7
Number of Offsprings	N_c	$2 \times round(P_c \times \frac{N_{Pop}}{2})$
Number of Mutants	N_m	$round\ (P_m \times N_{Pop})$
Mutation Rate	P_c	0,7
Mutation Percentage	P_m	0,3

Table 2. PSO program parameters

Parameter	Variable	Values
Cognitive component	C_1	1,5
Random numbers	$r_1;\ r_2$	[0,1]
Social component	C_2	2

5.1. Selection of the Objective Function

The selection of the best value of the selected fitness function is obtained using the optimization of the four objective functions. Adopting a genetic algorithm to turn the first strategy 3PI, the results are illustrated and well presented in Fig. 12.

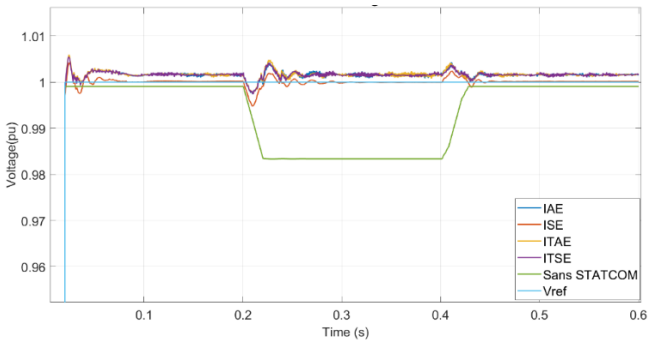

Fig. 12. Evolution of grid transient voltage value in (p.u) obtained from 4 objective functions (case of 3PI).

The simulation results show the importance and the efficiency of STATCOM for the best grid voltage profile stability under load variation in the electrical grid. The reactive power generated in the grid by the STATCOM into the electrical grid, to stabilize the grid voltage with a voltage drop (V < Vref) as clearly shown between the instant 0.2s and 0.4s.

We note that the ISE is visibly better than the IAE, ITAE, and ITSE in terms of time for establishing the steady state with a relatively small amplitude. This criterion is often used in the literature. The ISE criterion integrates the square of the error over time and ensures relatively low overrun. In the following parts of this section, the selected objective function ISE of grid voltage to tune the different strategies of STATCOM.

5.2. Simulation of STATCOM Control Strategies using EA

In this part, we will study 4 scenarios to control the STATCOM, such as the 3PI, 2PI+2PI in cascade, 2PI+FOPI, and 2PI+PIFOPI. The controllers are optimized by the application of the three studied EA algorithms (PSO, GA, and GA-PSO) to determine and fix the optimal values of the controllers in each scenario.

Table 3. Results of the optimal value of the selected fitness function optimized by the three algorithms.

Scenario	Optimal fitness function value		
	GA	PSO	GA-PSO
3PI	4.712×10^{-6}	8.815×10^{-6}	2.51×10^{-6}
2PI+2PI in cascade	1.583×10^{-6}	1.173×10^{-6}	1.194×10^{-6}
2PI+FOPI	1.233×10^{-6}	2.133×10^{-6}	1.132×10^{-6}
2PI+PIFOPI	1.161×10^{-6}	1.187×10^{-6}	1.105×10^{-6}

According to simulation results, Table 3 proves that the ISE of grid voltage is considerably reduced in each scenario with the combined method GA-PSO compared to GA and PSO. The comparative study between these three algorithms indicates and highlights that the hybrid GA-PSO approach yields superior results. It is also faster, more efficient, and robust than both PSO and GA algorithms, as it benefits from combining the strengths of each method.

Its global convergence performance knows GA, and it reaches the optimal value quickly due to the mutation operation. PSO performed in local convergence by searching for the best local position. It's represented in the velocity operation in the PSO process. That's why PSO reaches the best solution slowly compared to GA. Then GA-PSO combines both performances of GA and PSO and ameliorates the GA process. This proposed optimization method improves GA performance with the velocity operation of PSO.

Comparing the different simulated results of the four scenarios, the 2PI+PIFOPI strategy tuned and adjusted by the hybrid GA-PSO presents the best solution with a minimum fitness function value of 1.105×10^{-6}. As explained in Section 4, for the STATCOM control strategy, the internal current loop should be faster than two external voltage loops. That is obtained with a 2PI+PIFOPI strategy where the outer voltage loops are ensured with a two-cascaded PI controller and the inner current loop adopts the cascaded PI and FOPI controller.

As detailed in Section 3, the fractional order controller provides more dynamic performances than the linear PI. The cascaded PIFOPI combines the PI with linear and two fractional integral terms. The two-cascaded PI is characterized by double integral terms, which ameliorate the performance by reducing disturbances.

The disadvantages of PI include a larger maximum deviation (high overshoot), a longer response time (settling time), and a longer period of oscillation. The double integral term aims to improve the limitation of PI control by reducing the overshoot.

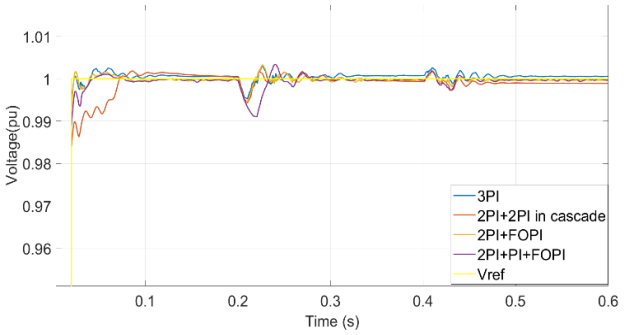

Fig. 13. Evolution of grid transient voltage value in (p.u) with different controllers tuned with GA.

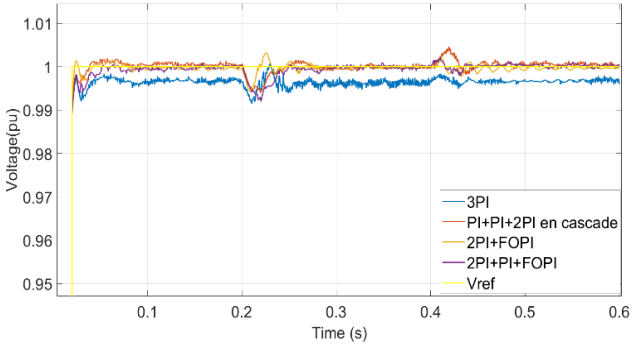

Fig. 14. Evolution of grid transient voltage value in (p.u) with different controllers tuned with PSO.

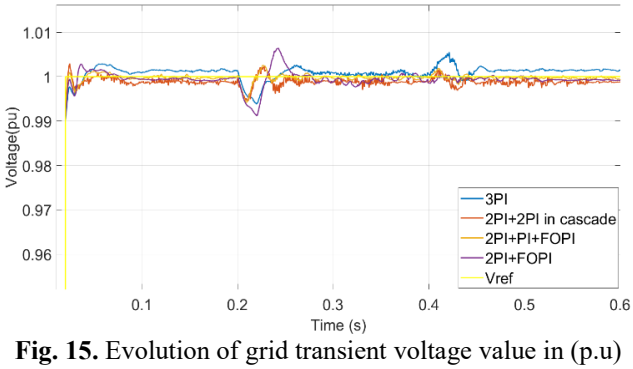

Fig. 15. Evolution of grid transient voltage value in (p.u) with different controllers tuned with GA-PSO.

Table 3 and Figures (13, 14, and 15) show that the 2PI+PIFOPI strategy turned by GA-PSO presents the performed control strategy with a minimum ISE equal to 1.105×10^{-6}.

Tables 4, 5, 6, and 7 present the optimal parameters of controls in all studied cases.

Table 4. Optimal parameters of the STATCOM controllers in scenario 1 (3PI)

Controller gains	GA	PSO	GA-PSO
k_{pAC} (AC Voltage)	62,3807	1,695	8,799
k_{iAC} (AC Voltage)	2021,577	2207,35	17,346
k_{pDC} (DC Voltage)	4,977	17,405	120,759
k_{pDC} (DC Voltage)	2317,038	170,604	8,944
k_p (Current)	0.,971	3,287	3,532
k_i (Current)	0,0192	81,198	0,555

Table 5. Optimal parameters of the STATCOM controllers in the scenario 2 (2PI+2PI in cascade)

Controller gains	GA	PSO	GA-PSO
k_{pAC} (AC Voltage)	8,94× 10^{-2}	0,82	8,908
k_{iAC} (AC Voltage)	351,45	305,2	683,444
k_{pDC} (DC Voltage)	6,0474	4,325	9,354
k_{pDC} (DC Voltage)	102,08	214,82	222,77
k_{p1} (Current)	2,223	0.213	1,965
k_{i1} (Current)	20,643	30,298	90,196
k_{p2} (Current)	0,430	93,377	2,355
k_{i2} (Current)	4,935	39,891	39,738

Table 6. Optimal parameters of the STATCOM controllers in scenario 3 (2PI+FOPI)

Controller gains	GA	PSO	GA-PSO
k_{pAC} (AC Voltage)	3,258	0,499	9,357
k_{iAC} (AC Voltage)	776,121	232,228	3647,08
k_{pDC} (DC Voltage)	10,513	453,029	16,927
k_{pDC} (DC Voltage)	554,032	445,419	91,677
k_p (Current)	2,971	2,408	3,513
k_i (Current)	180,72	41,352	92,266
Lambda (Current)	0,965	0,547	0,9

Table 7. Optimal parameters of the STATCOM controllers in scenario 4 (2PI+PIFOPI)

Controller gains	GA	PSO	GA-PSO
k_{pAC} (AC Voltage)	1,157	0,719	6,921
k_{iAC} (AC Voltage)	1561,835	325,134	1167,56
k_{pDC} (DC Voltage)	3,8046	638,516	21,957
k_{pDC} (DC Voltage)	192,2931	236,422	266,583
k_{p1} (Current)	6,25	478,014	1,144
k_{i1} (Current)	1,001	39,698	75,963
k_{p2} (Current)	0,557	475,214	3,629
k_{i2} (Current)	15,257	38,745	9,849
Lambda (Current)	5,49× 10^{-3}	0,447	0,846

5.3. Robustness Study of the Proposed Method's Performance

In this subsection, a parametric variation of impedance of different lines in the studied distributed grid was set to evaluate and measure the accuracy and robustness of the proposed algorithm. An elevation of 50% was applied in the model. The table below summarizes the simulation results and compares the ISE values.

Table 8. Simulation results of the best fitness function value (ISE) in the different scenarios under parametric uncertainties

Scenario		Optimal fitness function value (× 10^{-6})		
		GA	PSO	GA-PSO
3PI	Δ=0%	4.084	8.849	2.98
	Δ=50%	5.127	9.071	4.464
2PI+2PI in cascade	Δ=0%	1.583	1.173	1.194
	Δ=50%	2.059	3.758	1.283
2PI+FOPI	Δ=0%	1.233	2.133	1.132
	Δ=50%	1.79	2.247	1.141
2PI+PIFOPI	Δ=0%	1.161	1.187	1.105
	Δ=50%	1.27	1.452	1.113

Table 8 presents the simulation results of the robustness study and confirms the performance of GA and PSO proven in the previous four studied cases and scenarios.

These results justify the hybridization of GA and PSO, which is already presented in the first part of this section. Furthermore, the proposed method was compared with EA algorithms to verify its accuracy and better performance; the overall results are summarized in Table 11.

This test reveals that the GA-PSO algorithm is more robust than GA and PSO, the classical algorithms presented in this article, in minimizing the voltage deviation (ISE).

The simulation results once again confirm that the 2PI+PIFOPI scenario powered by GA-PSO provides the best performance, so it is the best control strategy for our STATCOM.

6. Conclusion

In this article, the PI and FOPI regulators are used to create scenarios for controlling the STATCOM voltage regulator. These scenarios, regulated by EA (PSO, GA, and combined GA-PSO), are used to solve the voltage control design problem of an electrical grid.

In the first part, the errors (IAE, ITAE, ITSE, and ISE) are compared to defend and justify the chosen objective function in this work. Furthermore, the simulation results (Figure 13) prove and demonstrate the effectiveness of STATCOM in ensuring the stability of the voltage in the electrical grid.

In the second part, the classical methods GA and PSO are tuned to improve their accuracy. The results clearly show their performance. The proposed GA-PSO algorithm uses a cascade structure. It minimizes the objective function (ISE). It also determines the optimal controller parameters for each strategy. The proposed GA-PSO optimization approach represents the best ISE values in the four scenarios and a good estimation of the controller parameters in these scenarios as indicated in the simulation results.

Comparing the simulation results, the 2PI+PIFOPI scenario optimized by the GA-PSO hybrid combination shows the best efficiency in STATCOM control. Such that, it presents an ISE value equal to 1.105×10^{-6} (Table 3).

Testing the robustness of the proposed strategy to control STATCOM shows that it maintains accuracy compared to other methods.

In perspective, a new STATCOM strategy can be explored by integrating renewable energies in the form of intermittent production.

Acknowledgements

No financial support was received for this study from public, commercial, or non-profit funding agencies.

Author Contributions

Khadija-Ikram Mahider was responsible for the formal analysis, investigation, methodology, software development, visualization, and original draft preparation. Reda Rabeh contributed to the conceptualization, investigation, project administration, resources, validation, and manuscript review and editing. Mohammed Ferfra was responsible for the conceptualization, investigation, project administration, resources, supervision, and validation. All authors contributed to the review and editing of the manuscript and have read and agreed to the published version of the manuscript.

Conflict of Interest

The authors declare that this work is entirely original, has neither been published previously nor submitted elsewhere for publication, and that there are no conflicts of interest associated with this research.

References

[1] K. K. Sharma, "Voltage regulation using FACT devices: a review", International Journal of Pure and Applied Mathematics, Vol. 119, No. 16, pp. 2207-2214, 2018.

[2] M. Mahdavian and F. H. Fesharaki, "The effect of shunt FACTS devices on voltage regulation in transmission lines", Signal Processing and Renewable Energy, pp. 85-94, June 2022.

[3] M. Peikherfeh, M. Abapour, M. P. Moghaddam, and A. Namdari, "Optimal allocation of FACTS devices for provision of voltage control ancillary services", 2010 7th International Conference on the European Energy Market, pp. 1-5, June 2010.

[4] M. Mahdavian, M. Janghorbani, E. Ganji, I. Eshaghpour, H. Hashemi-Dezaki, "Voltage regulation in transmission line by shunt flexible AC transmission system devices", 2017 14th International Conference on Electrical Engineering/Electronics, Computer, Telecommunications and Information Technology (ECTI-CON), pp. 107-110, June 2017.

[5] P. Kumar, "Application of FACT devices for voltage stability in a power system", 2015 IEEE 9th International Conference on Intelligent Systems and Control (ISCO), pp. 1-5, 2015.

[6] A. Saha, S. Ahmad, A. A. Soma, M. Z. A. Chowdhury, and A. A. Hossain, "Modelling and control of STATCOM to ensure stable power system operation", 2017 4th International Conference on Advances in Electrical Engineering (ICAEE), pp. 12-17, September 2017.

[7] R. H. Manoj, S. G. Kavita, and V. Jogi, "Voltage regulation of STATCOM using flexible PI control", 2017 2nd International Conference on Communication and Electronics Systems (ICCES), pp. 128-133, 2017.

[8] S. Choudhury, S. Sahoo, and S. K. Routray, "Voltage flicker compensation of STATCOM through novel bee colony optimization", 2020 International Conference on Smart Electronics and Communication (ICOSEC), pp. 1019-1024, November 2020.

[9] D. Kumar, V. Gupta, and R. C. Jha, "Implementation of FACTS devices for improvement of voltage stability using evolutionary algorithm", 2016 IEEE 1st International Conference on Power Electronics, Intelligent Control and Energy Systems (ICPEICES), pp. 1-6, 2016.

[10] S. Vadi, F. B. Gurbuz, S. Sagiroglu, and R. Bayindir, "Optimization of PI based buck-boost converter by particle swarm optimization algorithm", 2021 9th International Conference on Smart Grid (icSmartGrid), Setúbal, Portugal, pp. 295-301, 2021.

[11] I. N. Muisyo, C. M. Muriithi, and S. I. Kamau, "Enhancing low voltage ride through capability of grid connected DFIG based WECS using WCA-PSO tuned STATCOM controller", Heliyon, Vol. 8, No. 8, p. e09999, 2022, DOI: 10.1016/j.heliyon.2022.e09999.

[12] K. I. Mahider, M. Ferfra, and R. Rabeh, "Optimization of STATCOM PI controller parameters using the hybrid GA-PSO algorithm", 2023 IEEE 11th International Conference on Systems and Control (ICSC), Sousse, Tunisia, pp. 270-275, 2023.

[13] W. Rohouma, R.S. Balog, M.M. Begovic, A.A. Peerzada, "Capacitor-less D-STATCOM for voltage profile improvement in a SmartGrid distribution network with high PV penetration", 2022 10th International Conference on Smart Grid (icSmartGrid), Istanbul, Turkey, pp. 155-159, 2022.

[14] M. I. Mosaad, H. Ramadan, M. Aljohani, and M. El-Naggar, "Near-optimal PI controllers of STATCOM for efficient hybrid renewable power system", IEEE Access, Vol. 9, pp. 34119-34131, 2021, DOI: 10.1109/ACCESS.2021.3058081.

[15] A. Mohanty, M. Viswavandya, P.K. Ray, S. Mohanty, "Reactive power control and optimisation of hybrid offshore tidal turbine with system uncertainties", Journal of Ocean Engineering and Science, Vol. 1, No. 4, pp. 256-267, 2016, DOI: 10.1016/j.joes.2016.06.005.

[16] A. Idir, M. Kidouche, Y. Bensafia, K. Khettab, S. A. Tadjer, "Speed control of DC motor using PID and FOPID controllers based on differential evolution and PSO", International Journal of Intelligent Engineering and Systems, Vol. 11, No. 4, 2018, DOI: 10.22266/ijies2018.0831.24.

[17] S. Katoch, S. S. Chauhan, and V. Kumar, "A review on genetic algorithm: past, present, and future", Multimedia Tools and Applications, Vol. 80, pp. 8091-8126, 2021, DOI: 10.1007/s11042-020-10139-6.

[18] T. Bahi and A. Lakhdara, "Analysis of genetic and cuckoo search algorithms for MPPT in partial shaded", International Journal of Smart Grid-ijSmartGrid, Vol. 8, No. 1, pp. 35-40, 2024, DOI: 10.20508/ijsmartgrid.v8i1.329.g330.

[19] T.Y. Wu, Y.Z. Jiang, Y.Z. Su, W.C. Yeh, "Using simplified swarm optimization on multiloop fuzzy PID controller tuning design for flow and temperature control system", Applied Sciences, Vol. 10, No. 23, pp. 1-23, 2020, DOI: 10.3390/app10238472.

[20] M. A. Hossain, H. R. Pota, S. Aquartini, and A. F. Abdou, "Modified PSO algorithm for real-time energy management in grid-connected microgrids", Renewable Energy, Vol. 136, pp. 746-757, 2019, DOI: 10.1016/j.renene.2019.01.005.

[21] C. Aoughlis, A. Belkaid, I Colak, O. Guenounou, and M A. Kacimi, "Automatic and self adaptive P&O MPPT based PID controller and PSO algorithm", 2021 10th International Conference on Renewable Energy Research and Application (ICRERA), Istanbul, Turkey, pp. 385-390, 2021.

[22] R Raghutu, M Sankaraiah, R.S.S. Nuvvula, M. Venkatesh, "Dispatchable and non-dispatchable distributed generation reactive power coordination with reactive power-controlled devices using grey wolf optimizer", 2022 11th International Conference on Renewable Energy Research and Application (ICRERA), Istanbul, Turkey, pp. 33-41, 2022.

[23] H. Garg, "A hybrid PSO-GA algorithm for constrained optimization problems", Applied Mathematics and Computation, Vol. 274, pp. 292-305, 2016, DOI: 10.1016/j.amc.2015.11.001.